Progress In Electromagnetics Research C, Vol. 107, 97–111, 2021

A Novel Compact Wearable Antenna Design for ISM Band

Bo Yin, Ming Ye*, and Youhai Yu

Abstract—A compact wearable antenna operating at 2.45 GHz with a novel Electromagnetic Band Gap (EBG) structure as a reflector is proposed. The broadband monopole is used as the main radiator of the antenna, and the gradient feeder structure and etched slot on the ground are used to adjust the matching effect of the antenna port. The current path is extended, and the structure is made more compact by slotting the surface of the EBG cell. Then, a 3×3 EBG reflector is constructed and loaded to the bottom of the antenna to improve the antenna gain performance and reduces the specific absorptivity (SAR). A three-layer human model (skin-fat-muscle) has been built in High Frequency Structure Simulator (HFSS) to analyse the influence of human tissue on the wearable antenna system. Combined with the practical application background, the radiation performance of the system under bending is also explored. The simulation results show that the application of EBG reflector can increase the antenna gain by about 4.77 dBi and the front-to-back ratio by 17 dB, reduce SAR by more than 95%, and the overall size of the system is only $60.3 \times 60.3 \times 3.5\,\text{mm}^3$ (0.49λ). The antenna system has the characteristics of simple structure, small size, high gain, and low SAR value, which is of certain reference value for the research on the wearable antenna.

1. INTRODUCTION

China officially launches the commercial use of 5G in 2020. The real significance of 5G lies in opening the Internet of Things era of the Internet of Everything. As an important carrier of communication between people and things in the Internet of Things, wearable devices will become important terminal application devices [1]. Flexible electronic devices are widely used in the fields of information communication, biomedicine, and consumer electronics, etc. [2–4]. Because this technology can meet the needs of wearability, the flexible wearable technology derived from it has been widely studied. As a wearable device in the terminal equipment of the wireless communication system, antenna has become an important research hotspot in this field.

With the processing technology of flexible improving and free accessing to the ISM band around the world, Polyethylene Terephthalate (PET) [5], Polydimethylsiloxane (PDMS) [6], felt [7], textile fabrics [8], and other flexible materials have been widely used as antenna substrates. Patch, PIPF, monopole, and other antenna structures have been widely used in [9–11]. Methods such as loading short-circuit branches and loading lumped elements have been used in antenna miniaturization design [12, 13]. The conference paper [14] published by Salonen et al. in 1999 was the earliest literature on a wearable antenna. The authors proposed a wearable dual-frequency invert F antenna, which could be resonant at 900 MHz and 2.4 GHz, and proposed for the first time to explore the antenna radiation to the human body.

Since the wearable antenna works near the surface of the human body, the absorption of electromagnetic waves by human biological tissues will produce a heating effect. The electromagnetic

Received 19 October 2020, Accepted 16 November 2020, Scheduled 1 December 2020
* Corresponding author: Ming Ye (2057299173@qq.com).
The authors are with the College of Photoelectric Engineering, Chongqing University of Posts and Telecommunications, Chongqing 400065, China.

waves radiated from the back of the antenna need to be effectively suppressed to reduce the impact of antenna radiation on the human body. EBG structure can suppress electromagnetic waves from different angles in a certain frequency band, and its in-phase reflection characteristics can effectively reduce the antenna profile, so the structure is widely used in the fields of decoupling and low profile antenna design. In order to verify the improvement effect of EBG on antenna performance, a double-frequency wearable antenna loaded 3×3 EBG loop reflector was proposed in [15]. The authors verified the radiation performance of the antenna system under bending condition, and the simulation and test results showed that it had excellent bending performance and high gain, but the overall structure size was 120 mm, close to a wavelength. To demonstrate the working state of the antenna conformed with human body, Raad et al. proposed a claw shape coplanar waveguide feeding antenna loaded with a cross AMC reflector in [16], the polyimide as substrate material. The structure can greatly bend in the arm, and the measured result is good, but the overall gain of the antenna system is small, which is 4.8 dBi. Ref. [17] proposed a dual-frequency fabric antenna based on felt material. The authors simply analyzed the bending characteristics of the antenna, did not discuss the radiation effect of the antenna in combination with the human body model. In order to achieve further miniaturization, Ashyap and others used denim as EBG substrate material and designed a monopole antenna working at 2.4 GHz [8]. The EBG structure provided an antenna gain increase about 5.0 dBi and a front-to-back ratio increase of about 15 dB. Moreover, more than 95% SAR value was reduced, and the overall size of the system was about 0.38λ smaller. The simulation results verified the performance of the antenna when it was bent in different axial directions. Ref. [18] proposed a multiple antenna array based on an EBG structure, and the antenna layer, EBG layer, and floor layer were laminated into a whole. Multiple antenna units were connected in series. Meanwhile, the authors designed the matching network to improve the antenna matching effect and combined it with a human head model to verify its working performance. The antenna structure had good working performance, but its structural design was complex and required high processing technology.

In this paper, a miniaturized wearable antenna operating at $2.40 \sim 2.48$ GHz in the low frequency range of ISM is designed by using flexible polyimide as the substrate. A broadband monopole antenna is used as the main radiator, and the feed port matching effect is improved by using gradient feed [19] and loading ring matching slot [20] on a semi-ground structure. The size of the EBG structure is reduced by extending the surface current path through slits. Finally, its radiation performance of the antenna under different bending radians is verified by simulation. The antenna system has the characteristics of miniaturization, low profile, and low SAR value.

2. DESIGN OF ANTENNA SYSTEM

2.1. Antenna Design

A 2.45 GHz flexible microstrip antenna with microstrip line feed is designed. Microstrip antenna is characterized by a simple structure, good stability, and small size, which is suitable for the application environment of the wearable antenna in this paper. According to the design principle of a microstrip antenna, the operating frequency point is related to the equivalent current length and antenna medium substrate [21], which can be expressed as follows:

$$f = \frac{c}{2\pi L_e \sqrt{\varepsilon_e}} \tag{1}$$

where L_e is the equivalent current length, $L_e = L + 2\Delta L\,(L \gg \Delta L)$. ΔL is the antenna compensation length. ε_e is the effective dielectric constant. The antenna structure is shown in Fig. 1(c), which is composed of radiation patch, ground, gradient feeder, and dielectric substrate. The annular radiation patch is used to extend the operating bandwidth of the antenna so that the antenna system can meet the requirements after loading the EBG structure. Meanwhile, the gradient feeder is used at the feeding end to improve the matching effect, and the annular gap of the structure is designed on the ground to adjust the matching. The flexible polyimide material with dielectric constant of 3.5 and loss tangent of 0.002 is used as the dielectric substrate, and its thickness is 1.5 mm.

2.2. Structure and Simulation of Antenna

The antenna structure is derived from the improvement of a monopole antenna. The design process is shown in Fig. 1. In the initial structure (a), the circular patch is used as the radiation body, and the rectangular microstrip line is used for feeding. In order to further tune the frequency, the radiation patch is slotted in structure (b), and the feed structure is modified to gradient feeder according to the method in [19], so that the equivalent current path on the antenna surface can be extended, and the matching effect can be improved. At the same time, annular gaps are designed on the ground to further improve the antenna port matching.

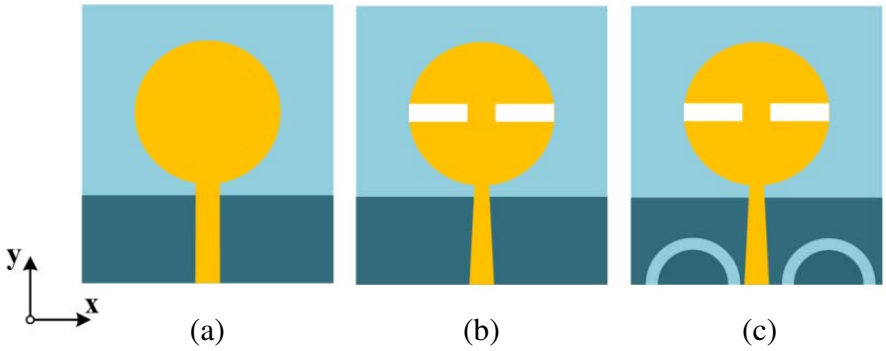

Figure 1. Process of antenna structure design. (a) The initial structure. (b) FM improvement. (c) Further improvement.

The S_{11} curves of the three modified antenna structures are shown in Fig. 2. It can be seen that the use of the annular gap and gradient feeder can improve the antenna matching effect obviously, and the use of antenna surface gap could reduce the resonant frequency point of the antenna to a certain extent. Fig. 3 is the radiation pattern of the antenna. The axial gain of the antenna is 2.2 dBi, and the front-to-back ratio at the frequency point is about 6 dB.

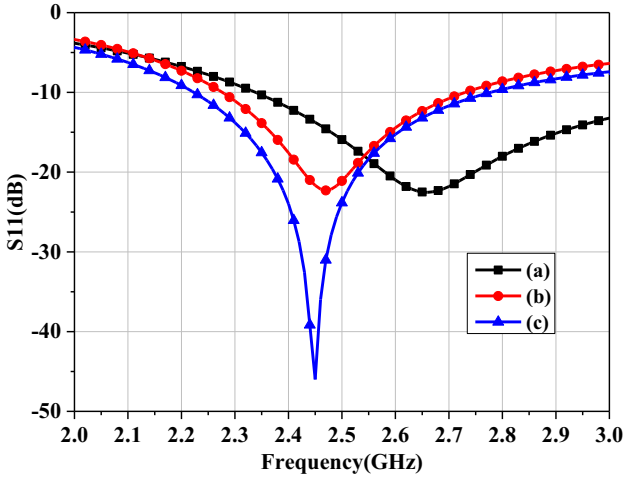

Figure 2. The magnitude of reflection co-efficient $|S_{11}|$ curves of different structure.

In order to explore the influence of different parameters on the radiation performance of the antenna structure, major radiation patch radius R_0 and ring inner radius R_1 on the ground are scanned to observe the changes of resonant frequency points under different values and verify the effects of corresponding structures. Finally, the antenna structure and size are shown in Fig. 4 and Table 1.

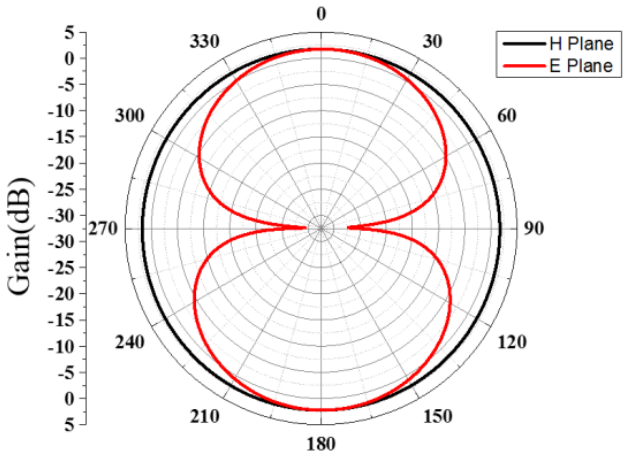

Figure 3. Radiation pattern of the antenna.

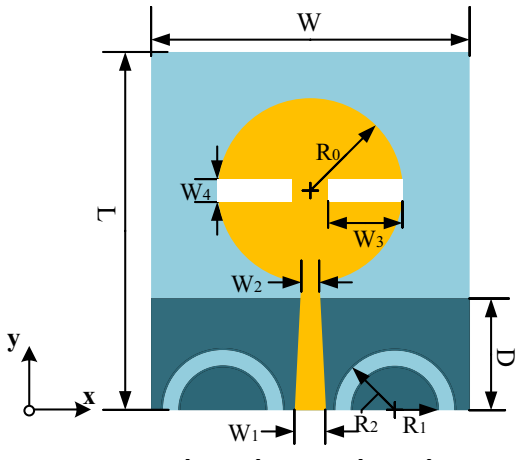

Figure 4. Configuration of the proposed antenna.

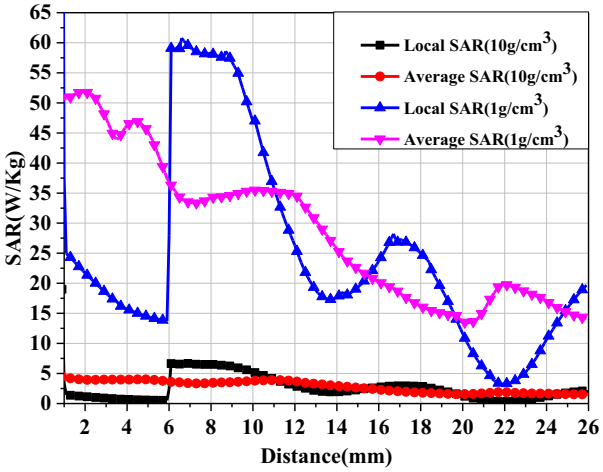

Figure 5. SAR value of the single antenna.

Table 1. Geometrical parameters of the proposed antenna.

W	35.0 mm	L	42.0 mm
W_1	4.4 mm	R_0	12.8 mm
W_2	3.6 mm	R_1	7.6 mm
W_3	8.0 mm	R_2	5.6 mm
W_3	8.0 mm	D	12.0 mm

Figure 5 shows the SAR value simulation after the human body model is loaded by a single antenna, and the human tissue density is set at 1 g/cm^3 and 10 g/cm^3, respectively. The simulation data show that the SAR values under the two standards are far greater than the standard value of 1.67 W/kg, which do not conform to the safety index of electromagnetic radiation. To reduce the SAR value, it is necessary to suppress the antenna backward radiation.

3. DESIGN OF WINDOW-TYPE EBG STRUCTURE

Due to the radiation of electromagnetic wave from the antenna in the negative direction, the heating effect will be produced on the human body, and some measures should be taken to suppress it. In this paper, a window-type EBG structure is proposed as shown in Fig. 6(c). The structure uses flexible polyimide as the substrate, whose thickness is 1.5 mm. Figs. 6(a) and (b) show the improvement process of the structure. According to Equation (2), the reduction of the resonant point can be achieved by increasing the structure's equivalent capacitance and inductance. The equivalent capacitance and inductance of the structure are increased by slotting its top patch and adding connecting units between the inner and outer rings, so that resonance frequency of the EBG structure is further moved to low frequency, with the final structure size of 19.9 mm ($0.16\lambda_e$). A 3×3 array is composed of the structure as the reflector of the antenna. The overall size of the reflector is $60.3 \times 60.3 \times 1.5\,\text{mm}^3$.

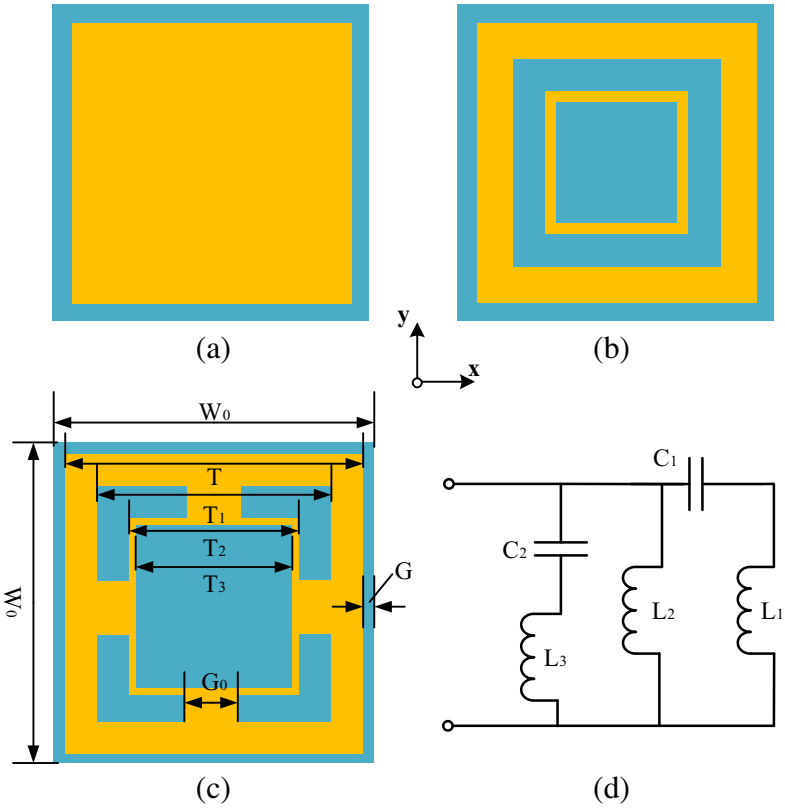

Figure 6. EBG structure and equivalent circuit diagram.

The equivalent circuit of window-type EBG structure is shown in Fig. 6(d). C_1 is the capacitance generated by the patch gap between two EBG units, and C_2 is the capacitance between the patch and ground. Compared with C_1, C_2 can be ignored. L_1 is the inductance generated by the surface patch of the unit structure, L_2 the inductance value increased after slotting, and L_3 the inductance generated by the contact between the substrate and the ground of the EBG unit. Compared with the inductance value L_1 on the surface, L_3 can be ignored [22].

According to the resonance theory, the resonance frequency points of EBG element structure can be expressed as formula (2):

$$f = \frac{1}{2\pi\sqrt{LC}} \tag{2}$$

where L and C are equivalent total inductance and total capacitance of the structure. After

simplification, $L = L_1 + L_2$, $C = C_1$. C_1 and L_1 can be approximated by Equations (3) and (4).

$$C_1 = \frac{T\varepsilon_0(1+\varepsilon_r)}{\pi}\cosh^{-1}\left(\frac{T+G}{G}\right) \tag{3}$$

$$L_1 = \frac{T\mu_0}{4\pi}\ln\left\{1+\frac{32H^2}{(T-T_1)^2}\left[1+\sqrt{1+\left(\frac{\pi(T-T_1)^2}{8H^2}\right)}\right]\right\} \tag{4}$$

where ε_0 and ε_r are the permittivity in vacuum and the relative dielectric constant, respectively. μ_0 is for permeability. T represents the external ring structure length. H is the substrate thickness of the unit. It can be seen from the above formula that when T of the unit structure is increased, capacitance C_1 and inductance L_1 will increase; the total capacitance C and total inductance L will also increase, and f, the resonant frequency point of the structure, will decrease. When the unit spacing G is reduced, the coupling capacitance C_1 between the units will increase, which can also reduce f. In order to verify the influence of different structure sizes on phase and resonance frequency points, the variables T and G in Equations (3) and (4), which affect the change of capacitance inductance value, are scanned by parameters to observe the change of phase points. Finally, with the 0° reflection of the structure in 2.45 GHz, ±90° phase interval is 2.40 to 2.50 GHz, and the unit structure size is shown in Table 2.

Table 2. Unit EBG structure size.

W_0	19.9 mm	T	19.5 mm
G_0	2.0 mm	T_1	15.2 mm
G	0.2 mm	T_2	12.7 mm
H	1.5 mm	T_3	11.6 mm

When the EBG structure is loaded to the bottom of the antenna, its in-phase reflection characteristics are mainly applied to reduce the structure profile and increase the gain value of the antenna's main radiation direction. In this paper using Floquet ports simulation method of its reflection phase characteristic, the simulation curve as shown in Fig. 7, with 0° reflection of the structure, can be seen in 2.45 GHz. ±90° phase interval is 2.40 to 2.50 GHz and covers low-frequency band of the ISM band. In this frequency band, the phase of the vertically incident electromagnetic wave and reflected wave are superimposed to enhance the antenna radiation effect.

4. SIMULATION OF THE ANTENNA SYSTEM

In order to verify the influence of EBG structure on antenna radiation performance, a 3×3 EBG array is loaded as a reflector at the bottom of the antenna for joint simulation. The system structure is shown in Fig. 8, with antenna thickness 0.5 mm and EBG reflector thickness 1.5 mm. The antenna body and reflector are supported by a piece of foam material with thickness of $d = 1.5$ mm, and the overall profile height is 3.5 mm ($0.029\lambda_e$).

Through simulation and optimization, the S_{11} curve and radiation pattern after loading EBG reflector are shown in Figs. 9(a) and (b), with the final structure of the overall size of only $60.3 \times 60.3 \times 3.5\,\text{mm}^3$ ($0.49\lambda_e$).

Set simulation center frequency 2.45 GHz. Because the monopole antenna and EBG reflector are very close, there is strong coupling between them. The phase of the reflected electromagnetic wave generated after irradiating the EBG reflector with the frequency of ±90° phase band will cancel each other out with the incoming electromagnetic wave. So it cannot effectively radiate to the free space, that is, the gain of antenna system decreases, or the effective radiation fails. On the other hand, due to the presence of the EBG reflector, the size of the antenna will no longer be the same as before the EBG reflector is loaded, and the center frequency point will shift to the high frequency. The presence of the antenna is also equivalent to adding a conductor structure near the EBG reflector, and the phase center of EGB will change accordingly. Therefore, it is necessary to fine-tune the two.

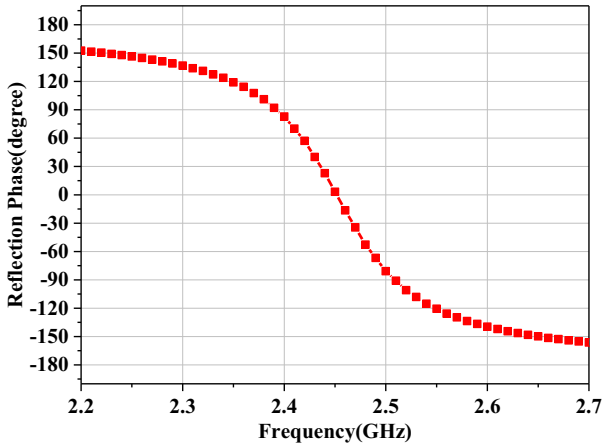

Figure 7. Reflection phase diagram of the unit structure.

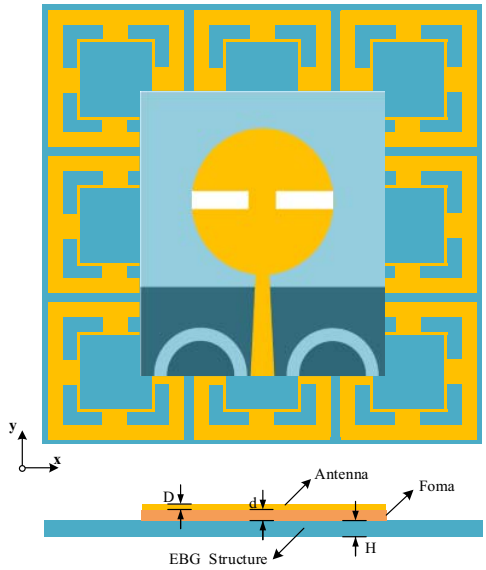

Figure 8. Antenna system loaded with EBG structure.

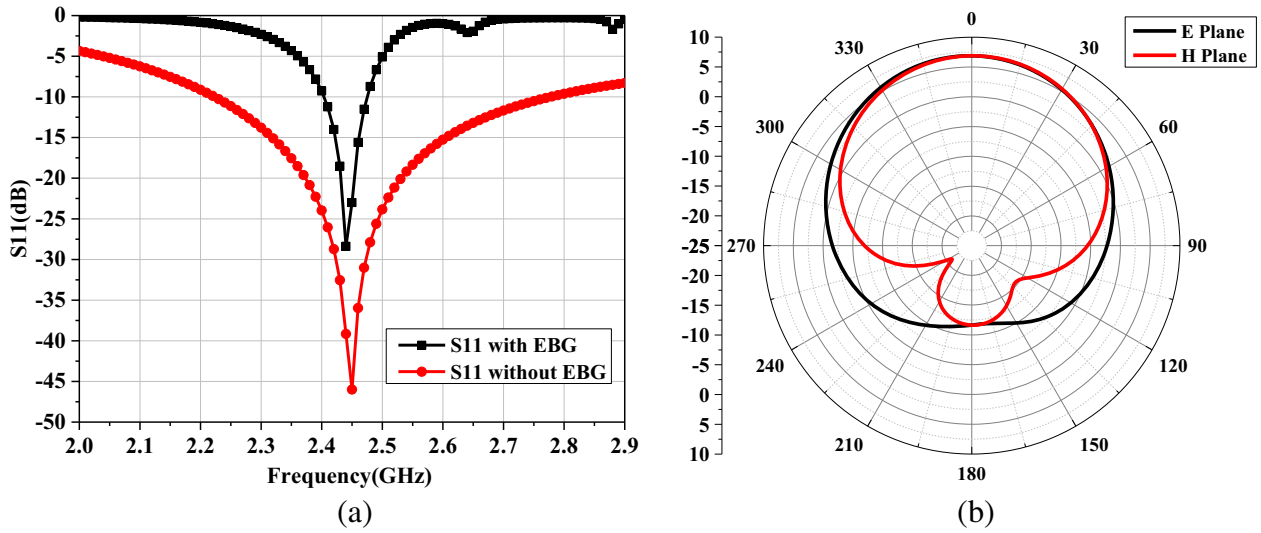

Figure 9. (a) S_{11} loaded with EBG structure. (b) Radiation pattern of the antenna.

As can be seen from Fig. 9(a), after loading the EBG reflector, antenna bandwidth is greatly reduced. -10 dB bandwidth of the composite structure is 2.41 $\sim$ 2.48 GHz, which can cover the 2.45 GHz band of ISM band. However, compared with the monopole antenna, the gain has been greatly improved, reaching 6.83 dBi and increasing about 4.6 dBi, and the front-to-back ratio is significantly increased by 20 dB, indicating that the backward radiation of the antenna is suppressed. Therefore, although the loading of the EBG reflector increases the overall size of the system, it effectively inhibits the backward radiation of the antenna, improves the gain, and reduces the SAR value of the antenna when it works near the human body surface.

4.1. The Simulation with Loading Human

Since the antenna system works on the human body surface, the electromagnetic wave radiated by the antenna will be absorbed by the human body and produce heating effect. Therefore, it is necessary to

Table 3. Electrical parameters of human tissues.

Tissue	ε	δ (°)	σ (Sm^{-1})	h/mm
Skin	38.007	0.283	1.49	1.0
Fat	5.280	0.145	0.11	5.0
Muscle	52.729	0.241	1.77	20.0

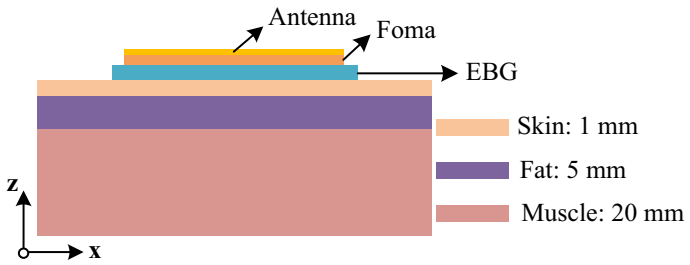

Figure 10. Structure model loaded the human tissue.

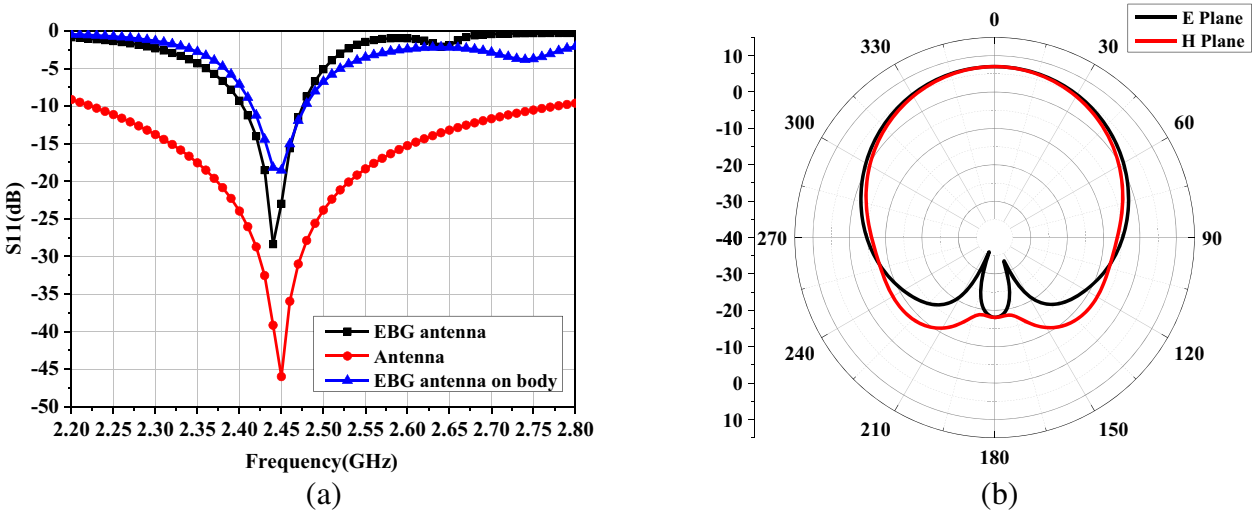

Figure 11. (a) Comparison of antenna S_{11}. (b) Radiation pattern with human model.

investigate the radiation characteristics of the antenna when it is placed on the human body surface. In 1999, IEEE defined the specific absorption rate of 1.67 W/kg as the upper limit of electromagnetic waves absorbed by the human body. Referring and using the relevant electrical parameters of human tissue structure in [20] (shown in Table 3), a three-layer structure model is loaded at the bottom of the antenna structure to simulate human skin, fat, and muscle tissues, respectively, and joint simulation is conducted with the antenna system, with the model structure as shown in Fig. 10.

Figure 11(a) shows the comparison of S_{11} in different states. It can be seen that the antenna matching will deteriorate after loading the human body model, and the operating frequency point will drift to some extent, but the −10 dB bandwidth is still in the ISM frequency band, meeting the working requirements. Fig. 11(b) shows the radiation pattern after loading the human body model. Compared with Fig. 9(b), it is found that the gain in the axial direction of the antenna system is increased by about 0.15 dBi, reaching 6.97 dBi. At the same time, the radiation performance of E plane is improved, and the back lobe is significantly reduced. Fig. 12 is the comparison of front-to-back ratio in different conditions. After loading the human body, front-to-back ratio has a further improvement and is greater than 25 dB. Figs. 13(a) and (b) show the SAR value distributions of the antenna before and after loading the EBG.

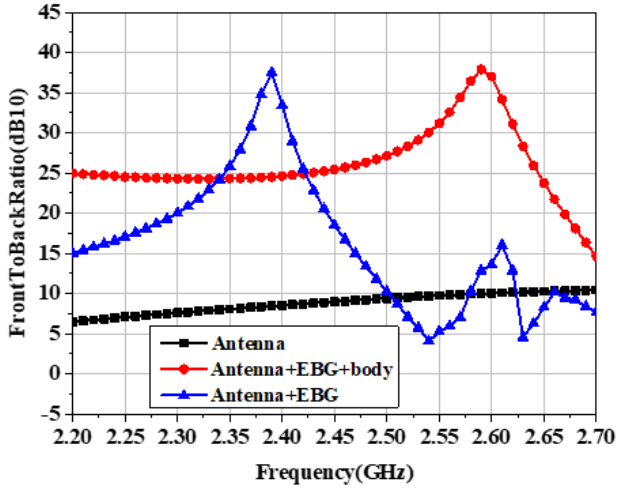

Figure 12. The contrast of front-to-back ratio.

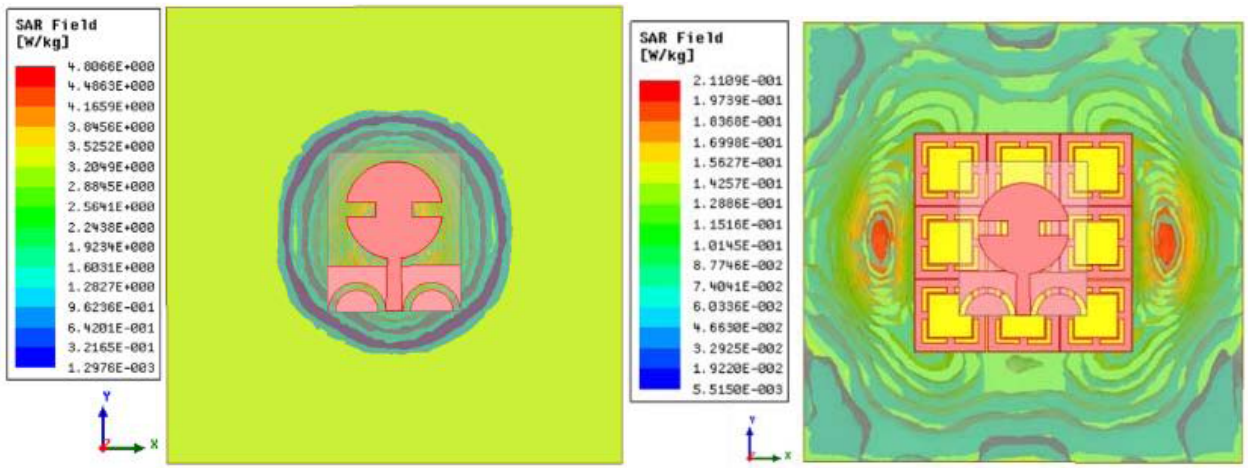

Figure 13. (a) SAR distribution of human tissue when a single antenna is radiated. (b) SAR distribution of human tissue after loading the EBG.

As can be seen from Fig. 13(a), the areas where human tissues absorb the most electromagnetic waves are on both sides of the non-feeding end of the antenna. The simulation contrast tissues with 1 g/cm^3 density and 10 g/cm^3 SAR values, respectively, of indicators as shown in Fig. 14. It can be seen that the maximum SAR values under these two densities are 0.24 W/kg and 0.024 W/kg, respectively, far less than the SAR value of standard of international definition. Compared with Fig. 5, it is found that the SAR value decreases by more than 95% after loading EBG, indicating that the loading of EBG reflector structure has an obvious inhibitory effect on the backward radiation of the antenna.

The electrical parameters related to the antenna system are compared with other antenna structures of the same type in the references, and the results are shown in Table 4.

4.2. Simulation of Antenna System Bending

When the flexible antenna is affected by external forces, the center frequency point will drift. In order to verify the stability of the antenna structure, a cylindrical model similar to the electrical parameters of human tissues is used to simulate the conformal state of the antenna when worn on the human surface.

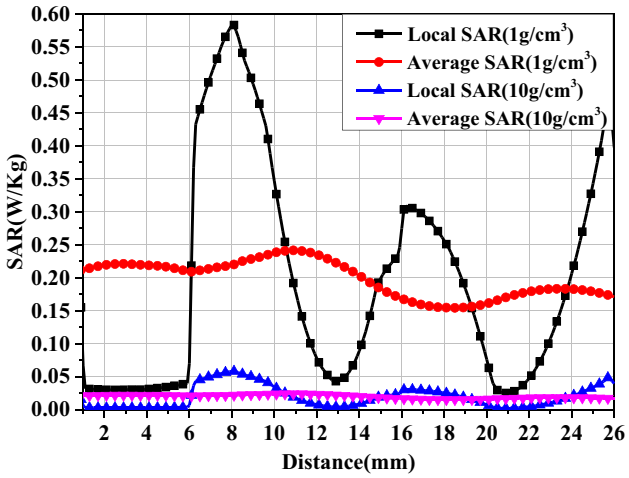

Figure 14. Simulation of SAR values loaded with EBG.

Table 4. Comparison of different wearable structure indicators.

Ref.	Number of unit cell	Frequency (GHz)	Gain (dBi)	Dimension (mm^3)	SAR (W/Kg)	Reflected plane	Substrate type
[23]	$3*3$	2.45	4.8	$65.7 \times 65.7 \times 3.3$	0.683	AMC	Polyimide/flexible
[24]	$2*2$	2.45	6.55	$60 \times 60 \times 2.4$	0.055	EBG	Felt/flexible
[15]	$3*3$	2.45/5.80	N/A	$120 \times 120 \times 4.3$	0.127	EBG	Jeans/flexible
[25]	$3*3$	2.45	7.3	$81 \times 81 \times 4$	0.554	EBG	Nylon/flexible
[26]	$3*3$	2.45	6.4	$83 \times 89 \times 3.0$	0.29	AMC	Rogers3003/flexible
This paper	$3*3$	2.45	6.93	$60.3 \times 60.3 \times 3.5$	0.24	EBG	Polyimide/flexible

According to Equation (5), the larger O_1 is, the smaller β is. The relationship between the curve radian β and the radius of curvature radius O_1 is as follows:

$$W = \beta\,(O_1 + H) \tag{5}$$

where W is the width of the substrate, and H is the thickness of the substrate. The antenna system is bent with O_1 of 100 mm, 120 mm, and 140 mm, respectively, and its working conditions are observed through simulation. The antenna system under different β is shown in Fig. 15(a). The S_{11} curve of the antenna under the bending state is shown in Fig. 15(b).

As can be seen from Fig. 15(b), with the decrease of O_1, β gradually increases; the resonant frequency point will move to low frequency; and the greater β is, the more obvious the frequency deviation is. However, because the overall size of the antenna system is smaller than that of the human limb, the actual wear bending radian is not large; the resonant frequency shift is small; the structure can satisfy the requirement.

4.3. Antenna Fabrication and Measurement

In order to verify the previous design, a prototype of wearable antenna is fabricated. The physical photograph of the antenna in the bending state is shown in Fig. 16(a). The antenna is placed at 1.5 mm above the EBG reflector and filled with foam material between the antenna and the EBG reflector. For the convenience of the antenna in the human body surface, a 15 cm long RF tieline is used to extend the feeder port. Then, the antenna loaded with an EBG reflector is placed on the body surface of a

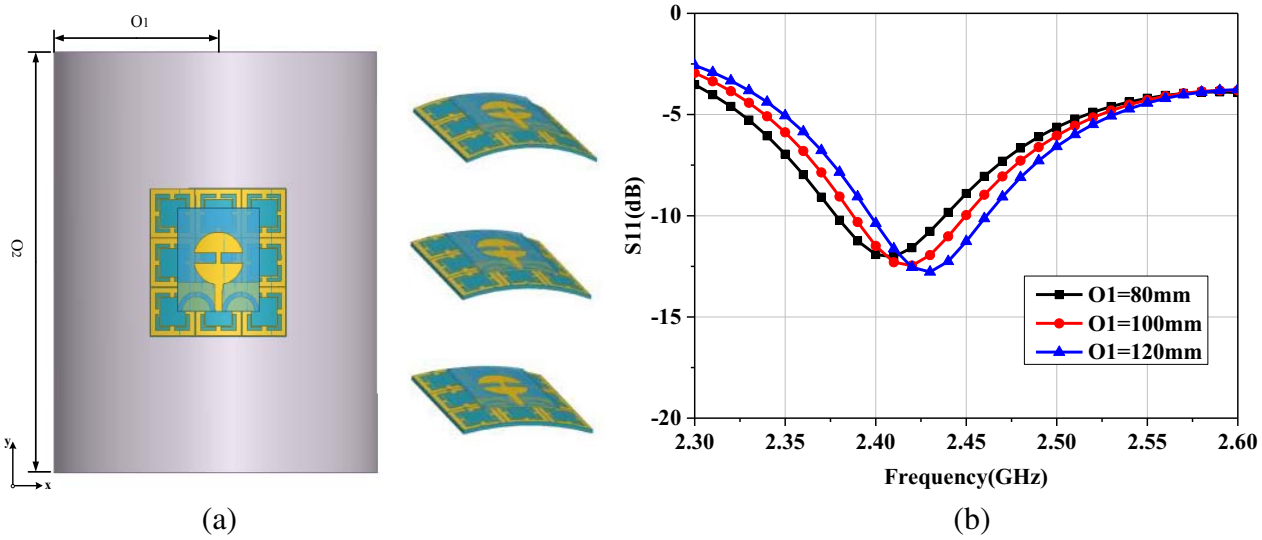

Figure 15. (a) Antenna structure under different β. (b) S_{11} under different β.

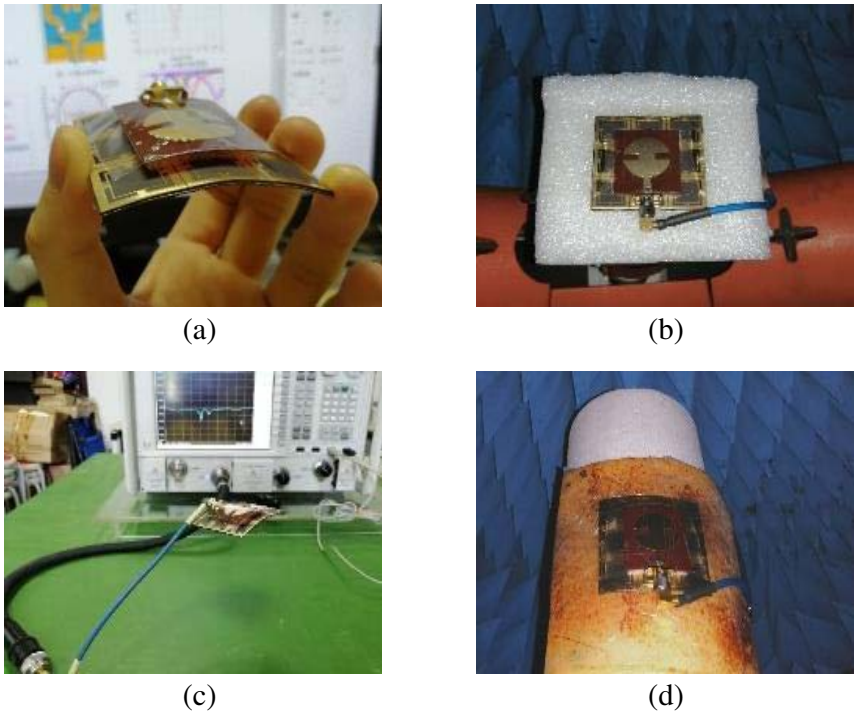

Figure 16. Physical structure and test drawings of antenna. (a) The bending of the antenna. (b) Radiation test of plane state. (c) Radiation test of bending state. (d) Test with biological tissue.

body (height 175 cm weight 65 kg of male) to observe its S parameters. The radiation pattern and gain of the wearable antenna system are also measured in the anechoic chamber of the SATIMO16 probe in our university. Meanwhile, as shown in Fig. 16(d), a 26 mm thick pork with a fat layer and a muscle layer is placed under the antenna system for combined test to verify the influence of human tissue on the antenna radiation.

S_{11} parameters of antenna radiation under plane state and bending state are tested, respectively, and the test results are compared with the simulation values, as shown in Fig. 17.

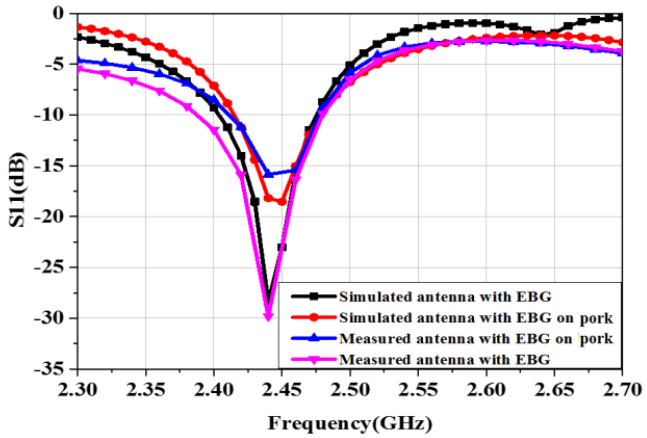

Figure 17. Comparison of plane state and bending state.

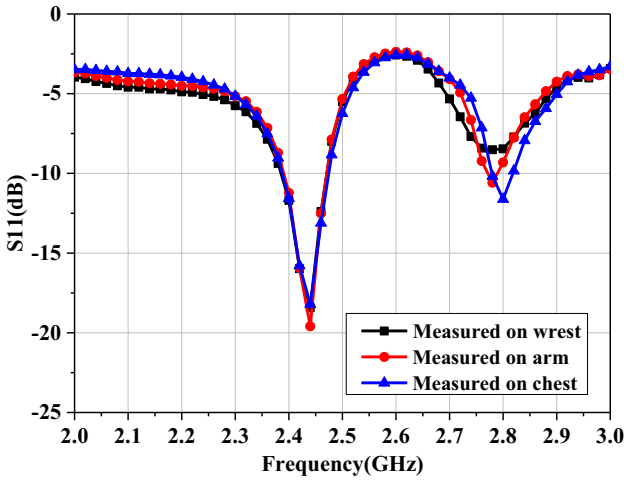

Figure 18. S_{11} of antenna measured on different parts of the body.

It can be seen that the port matching effect deteriorates after human tissues are loaded. S_{11} at the resonant frequency point is -19 dB, but it is still in the operating frequency band, and the measured value is in good agreement with the simulation value. In order to compare the radiation performance of the antenna working on the human body surface, the antenna structure is attached to different parts of the human body for measuring, and the results are shown in Fig. 18.

The test results show that when the antenna system is loaded in different parts of the human body, the radiation performance is relatively stable; the resonant frequency point of the antenna does not shift; the limb parts have little influence on the radiation of the antenna; and the backward radiation of the antenna is effectively isolated and less affected by human tissues. The radiation gain is shown in Fig. 19.

It can be seen that there is a small error between the measured and simulated values, which may be caused by the SMA port welding process, measurement error of microwave anechoic chamber, etc. After loading the EBG reflector, the band gain is greater than 6.5 dBi. When the wearable antenna with the EBG structure is placed on the human chest, the test results of the gain are in good agreement with the simulation results, but they are lower than the values when it is tested alone. When the wearable antenna with EBG structure is placed on the pork surface, the measured gain reduction value is about 0.6 dBi lower than the simulation value. On the whole, the state is relatively stable when it works in different parts of human body.

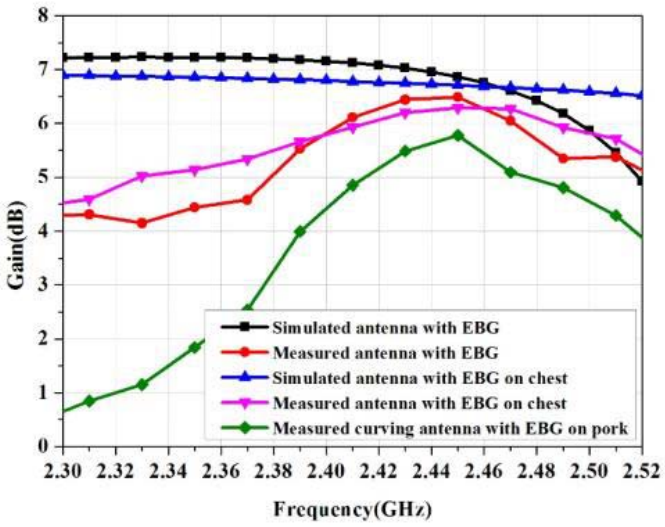

Figure 19. Gain's comparison of plane state and bending state.

5. CONCLUSION

This paper introduces a wearable antenna system that works with 2.45 GHz in ISM band. In the antenna design, gradient feeding and annular gap etched on the floor are used to adjust the matching of the feeding port. In the design of window-type with EBG structure, the surface current path is extended and miniaturized by surface slotting. A 3×3 EBG array is loaded as a reflector at 1.5 mm at the bottom of the antenna, and the overall size of the system is less than $1/2\lambda_g$. The simulation results show that a window-type of the application of EBG reflector can effectively increase the antenna gain, improve front-to-back ratio, and the reduction efficiency of human SAR value reaches more than 95%, which is far lower than the international standard. At the same time, the working condition of the antenna system under the bending state is simulated, and the results show that under small amplitude bending condition, the antenna can still maintain good radiation characteristics. Finally, the antenna structure is processed and measured, and the measured values of gain and return loss are in good agreement with the simulated values. Therefore, the system is characterized by small size, simple structure, good stability, and low SAR value, which are of reference value for the research on the wearable antenna.

REFERENCES

1. Thakkar, Y., X. Lin, Y. Chen, F. Yang, R. Wu, and X. Zhang, "Wearable monopole antennas for microwave stroke imaging," *European Conference on Antennas and Propagation, EuCAP*, 1–5, 2019.
2. Wagih, M., Y. Wei, A. Komolafe, et al., "Reliable UHF long-range textile-integrated RFID tag based on a compact flexible antenna filament," *Sensors*, Vol. 20, 12, 2020.
3. Soontornpipit, P., "Flexible graphene Waffle-typed antenna for skin-typed medical applications," *International Electrical Engineering Congress, iEECON*, 1–4, 2018.
4. Tariq, F., Q. Amjad, A. Kamran, A. Hassan, and R. Karim, "A flexible antenna on cost-effective PEN substrate for sub-6 GHz 5G wireless transceivers," *International Conference on Frontiers of Information Technology, FIT*, 89–895, 2019.
5. Simorangkir, R. B. V. B., Y. Yang, K. P. Esselle, and B. A. Zeb, "A method to realize robust flexible electronically tunable antennas using polymer-embedded conductive fabric," *IEEE Trans. Antennas Propag.*, Vol. 66, No. 1, 50–58, Jan. 2018.

6. Simorangkir, R. B. V. B., A. Kiourti, and K. P. Esselle, "UWB wearable antenna with a full ground plane based on PDMS-embedded conductive fabric," *IEEE Antennas and Wireless Propagation Letters*, Vol. 17, No. 3, 493–496, Mar. 2018.
7. Hussin, E. F. N. M., P. J. Soh, M. F. Jamlos, et al., "Wideband microstrip-based wearable antenna backed with full ground plane," *International Journal of RF and Microwave Computer-Aided Engineering*, Vol. 29, No. 7, 1–12, Mar. 2019.
8. Ashyap, A. Y. I., et al., "Compact and low-profile textile EBG-based antenna for wearable medical applications," *IEEE Antennas and Wireless Propagation Letters*, Vol. 16, 2550–2553, Jul. 2017.
9. Atanasova, G. L. and N. T. Atanasov, "Impact of electromagnetic properties of textile materials on performance of a low-profile wearable antenna backed by a reflector," *2020 International Workshop on Antenna Technology, iWAT*, 1–4, 2020.
10. Sultana, S., R. R. Hasan, T. Kumar Mondal, R. Tariqul Hasan Tusher, and S. Zabin, "Performance analysis of body implantable PIFA at different substrate material," *2017 4th International Conference on Advances in Electrical Engineering, ICAEE*, 68–73, 2017.
11. Kulkarni, J. S. and R. Seenivasan, "A novel, very low profile, dual band inverted 'E' monopole antenna for wireless applications in the laptop computer," *IEICE Electronics Express*, Vol. 16, No. 10, 20190157, 2019.
12. Nechayev, Y. I., P. S. Hall, and Z. H. Hu, "Characterisation of narrowband communication channels on the human body at 2.45 GHz," *IET Microwaves, Antennas Propag.*, Vol. 4, No. 6, 722–732, Jun. 2010.
13. Rowe, W. S. T. and R. B. Waterhouse, "Reduction of backward radiation for CPW fed aperture stacked patch antennas on small ground planes," *IEEE Trans. Antennas Propag.*, Vol. 51, No. 6, 1411–1413, Jun. 2003.
14. Salonen, P., L. Sydanheimo, M. Keskilammi, and M. Kivikoski, "A small planar inverted-F antenna for wearable applications," *Digest of Papers. Third International Symposium on Wearable Computers*, 95–100, 1999.
15. Zhu, S. and R. Langley, "Dual-band wearable textile antenna on an EBG substrate," *IEEE Trans. Antennas Propag.*, Vol. 57, No. 4, 926–935, Apr. 2009.
16. Raad, H. R., A. I. Abbosh, H. M. Al-Rizzo, and D. G. Rucker, "Flexible and compact AMC based antenna for telemedicine applications," *IEEE Trans. Antennas Propag.*, Vol. 61, No. 2, 524–531, Feb. 2013.
17. Yan, S., P. J. Soh, and G. A. E. Vandenbosch, "Low-profile dual-band textile antenna with artificial magnetic conductor plane," *IEEE Trans. Antennas Propag.*, Vol. 62, No. 12, 6487–6490, Dec. 2014.
18. Alqadami, A. S. M., K. S. Bialkowski, A. T. Mobashsher, and A. M. Abbosh, "Wearable electromagnetic head imaging system using flexible wideband antenna array based on polymer technology for brain stroke diagnosis," *IEEE Trans. Biomedical Circuits and Systems*, Vol. 13, No. 1, 124–134, Feb. 2019.
19. Kuang, B., "Analysis and design of sensitively loaded miniaturized and wideband antennas," Xidian University, Xi'an, 2013.
20. Arora, T., S. Gupta, K. K. Singh, and N. Kumar, "Effect of feedline tapering on the performance of super ultra-wideband circular monopole microstrip antenna," *2017 IEEE International Conference on Antennas Innovations & Modern Technologies for Ground, Aircraft and Satellite Applications, iAIM*, 1–4, 2017.
21. Xie, Z. C., Y. Huang, Z. Q. Wang, et al., "Design and sensing characteristics of 2.45 GHz flexible microstrip antenna," *Journal of Jilin University (Science edition)*, Vol. 57, 166–171, 2019.
22. Wang, M., et al., "Investigation of SAR reduction using flexible antenna with metamaterial structure in wireless body area network," *IEEE Trans. Antennas Propag.*, Vol. 66, No. 6, 3076–3086, Jun. 2018.
23. Raad, H. R., A. I. Abbosh, H. M. Al-Rizzo, and D. G. Rucker, "Flexible and compact AMC based antenna for telemedicine applications," *IEEE Trans. Antennas Propag.*, Vol. 61, No. 2, 524–531, Feb. 2013.

24. Ashyap, A. Y. I., et al., "Highly efficient wearable CPW antenna enabled by EBG-FSS structure for medical body area network applications," *IEEE Access*, Vol. 6, 77529–77541, 2018.
25. Gao, G., B. Hu, S. Wang, and C. Yang, "Wearable circular ring slot antenna with EBG structure for wireless body area network," *IEEE Antennas and Wireless Propagation Letters*, Vol. 17, No. 3, 434–437, Mar. 2018.
26. El Atrash, M., M. A. Abdalla, and H. M. Elhennawy, "A wearable dual-band low profile high gain low SAR antenna AMC-backed for WBAN applications," *IEEE Trans. Antennas Propag.*, Vol. 67, No. 10, 6378–6388, Oct. 2019.